Comparing 2D and 3D acoustic full-waveform inversion of the Snowflake baseline VSP dataset

Introduction

Carbon capture and storage (CCS) is critical technology for greenhouse gas reduction in which CO_2 is stored in the subsurface geological traps. In a CCS project, time-lapse seismic monitoring is commonly employed due to its capacity to delineate underground structural images with high resolution. Effective use of seismic inversion technology, by which these images are constructed from seismic data, remains an active area of research. To address these challenges, the Containment and Monitoring Institute Field Research Station (CaMI-FRS) was established. The Consortium for Research in Elastic Wave Exploration Seismology (CREWES) collaborated with Carbon Management Canada (Lawton et al., 2017) to acquire a unique 3D vertical seismic profile (VSP) dataset at CaMI-FRS, referred to as the Snowflake. This dataset has recently been expanded to become a full 4D VSP, and CREWES now exclusively owns it. Monitoring through full-waveform inversion (FWI) of these data is actively under examination at present (Cai et al., 2022; Eaid et al., 2023). However, most analyses have been conducted in 2D azimuthal slices. In this study, we apply 3D acoustic full-waveform inversion to the baseline dataset and aim to evaluate the potential importance of 3D FWI. Comparisons between 2D and 3D acoustic FWI, with all other factors essentially unchanged, decisively demonstrate the role of 3D.

The CREWES Snowflake dataset

The CaMI FRS is established to develop and validate the applicability of CO_2 monitoring technologies (Eaid et al., 2023). The basal belly river sandstone (BBRS) layer, located at a depth of 295-302 m, is a very thin injection layer with a thickness of 7 m (Macquet et al., 2019). In 2018, in collaboration with the CaMI-FRS, CREWES acquired 3D Snowflake baseline, walk-away and walk-around VSP. It comprises a total of 12 shot lines placed at 15-degree intervals, centered on the Geophysics well (Hall et al., 2018). In the geophysics well, 3C accelerometers are deployed from the surface to a depth of 324 m at 1-2 m intervals (Figure 1). There are four main lines (lines 1, 4, 7 and 10), which have enough number of sources. We use only the data recorded up to 0.3 seconds from the vertical component among the 3C components acceleration data (Figure 2). Figure 3 represents the original well-log data (Hu et al., 2022) and smoothed version to build initial velocity model. The model size is set to $1{\times}1{\times}0.35$ km^3 with 5 m grid spacing for 3D FWI considering the maximum offset of field data (Figure 3).

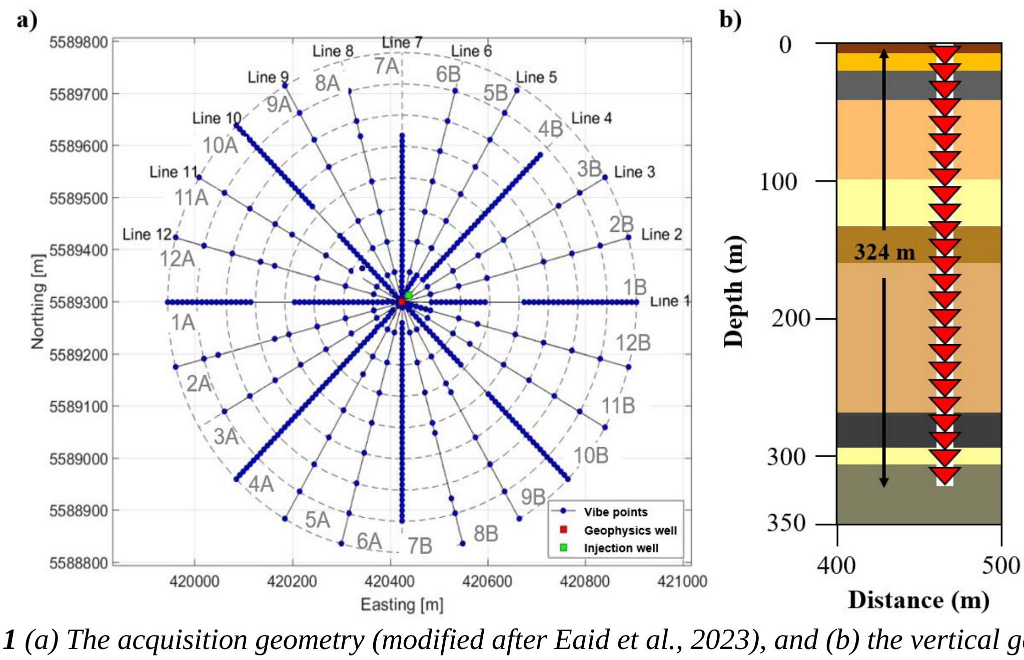

Figure 1 (a) The acquisition geometry (modified after Eaid et al., 2023), and (b) the vertical geometry of the 3D walk-away and walk-around VSP survey referred as Snowflake I. The red triangles represent receivers, and a total of 291 3C geophones are installed in the geophysics well.

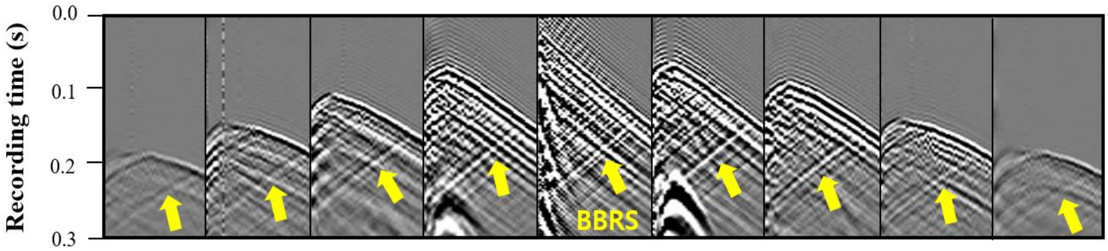

Figure 2 *Vertical components of Snowflake I data extracted along Line 1 in Figure 1.*

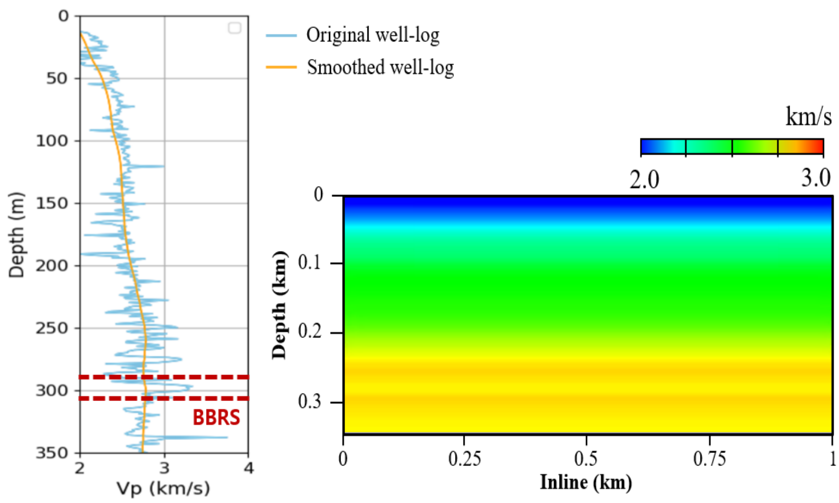

Figure 3 *The depth profile of P-wave velocity from the well-log and the cross-sectional view of the initial velocity model obtained from smoothed well-log.*

3D acoustic FWI with global correlation norm

FWI has been widely used to estimate underground properties by minimizing the residual through iterative processes (Tarantola, 1984). While there have been significant advancements in enhancing the adaptability of 3D acoustic FWI to field seismic data, it still faces several challenges: (I) amplitude mismatching, (II) poor S/N ratio and (III) computational costs. To address these challenges, we employ the global correlation norm (GCN) as the objective function between modelled (u) and field (d) data in the time domain, as expressed by (Choi and Alkhalifah, 2012),

$$E(\mathbf{m}) = \sum_s \sum_r \left[-\hat{u}(s,r,\mathbf{m}) \cdot \hat{d}(s,r) \right], \tag{1}$$

where

$$\hat{u}(s,r,\mathbf{m}) = \frac{u(s,r,\mathbf{m})}{\left\| u(s,r,\mathbf{m}) \right\|} \quad \text{and} \quad \hat{d}(s,r) = \frac{d(s,r)}{\left\| d(s,r) \right\|}. \tag{2}$$

The terms s and r denote the source and receiver, respectively. The variable $\mathbf{m}$ represents the model parameter, indicating the subsurface P-wave velocity. In our case, the modelled and field data correspond to the vertical acceleration components of the wavefields. According to Choi and Alkhalifah (2012), GCN exhibits similarities to phase-only inversion in the frequency domain. Furthermore, the normalization introduced in equation (2) allows for the automatic mitigation of the impact of strong noisy traces. Upon calculating the partial derivative with respect to the model parameter, the gradient direction at i^{th} nodal point is expressed as follows:

$$\frac{\partial E(\mathbf{m})}{\partial m_i} = \sum_s \sum_r \left[\frac{\partial u(s,r,\mathbf{m})}{\partial m_i} \cdot b(s,r,\mathbf{m}) \right], \tag{3}$$

with the adjoint source given by

$$b(s,r,\mathbf{m}) = \frac{1}{\|u(s,r,\mathbf{m})\|}\left\{\hat{u}(s,r,\mathbf{m})[\hat{u}(s,r,\mathbf{m})\cdot\hat{d}(s,r)] - \hat{d}(s,r)\right\}. \tag{4}$$

Due to the computational costs associated with equation (3), we employ the adjoint-state method (Plessix, 2006) to reduce the number of forward modelling. Specifically, for 3D acoustic FWI, we use the boundary value reconstruction (Xu et al., 1995) to reduce storing huge source wavefields.

Acoustic FWI for Snowflake data

As shown in Figure 1, walk-away and walk-around VSP acquisition of CaMI-FRS field data enables the approximation of 2D FWI along each walk-away line. Therefore, we compare 2D acoustic FWI results for each main line (1, 4, 7 and 10) and 3D acoustic FWI with entire dataset. The data has been muted before first arrivals and only vertical acceleration recorded up to 0.3 seconds is used. To detect thin BBRS layer with a thickness of 7 m, we use the ricker wavelet, whose peak frequency is 100 Hz, considering vertical resolution. Both 2D and 3D FWI are conducted using the same parameters, except for boundary value reconstruction. We apply pseudo-Hessian (Shin et al., 2001) and gradient direction normalization at each iteration. Additionally, to mitigate vertical noise around the borehole, we smooth the gradient direction only along the lateral directions using a smoothing window of 25 m for each direction. The total iteration is 15 with a fixed step length of 0.02 km/s.

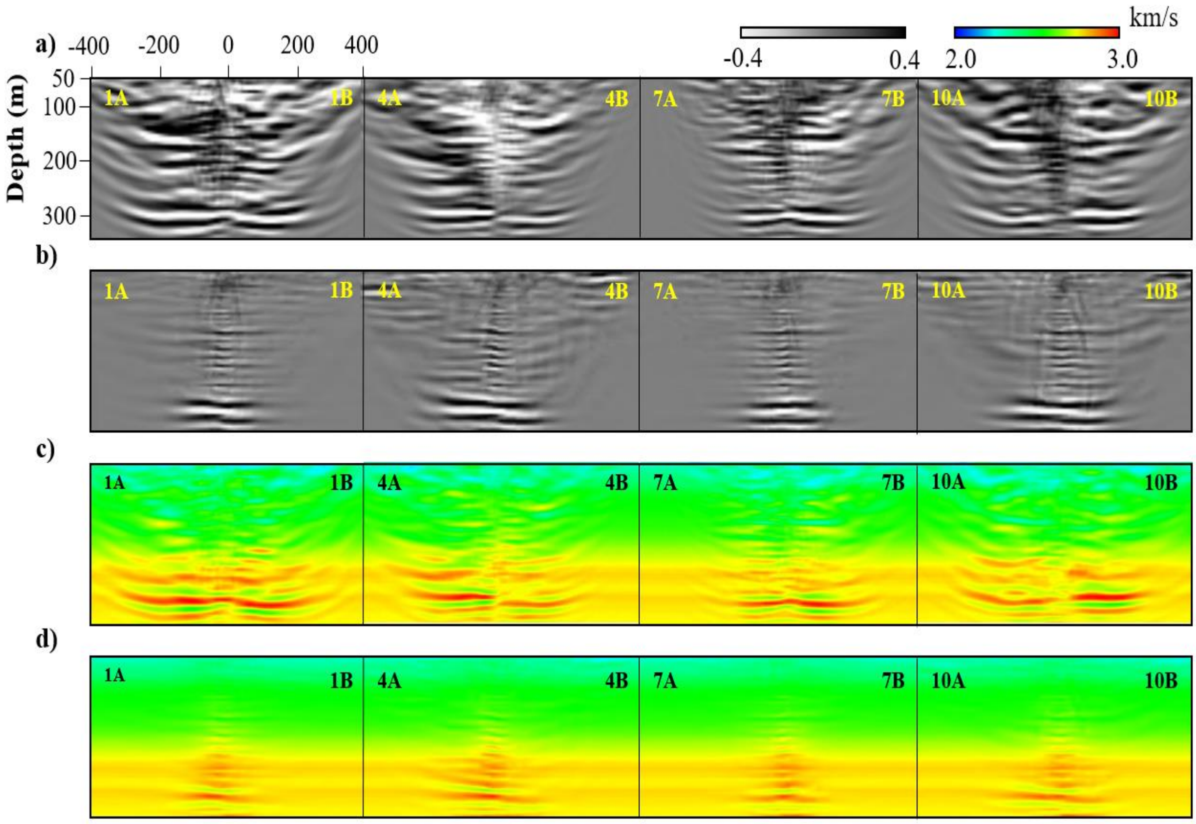

Figure 4 *The first-iteration gradient direction of (a) 2D FWI and (b) 3D FWI, and final inverted model of (c) 2D FWI and (d) 3D FWI. For comparison, the 3D FWI results are extracted along main shot lines (Lines 1, 4, 7, and 10). A and B indicate ends of each survey line (Figure 1).*

Figure 4 represents the first-iteration gradient direction and the final inverted model of 2D FWI and 3D FWI. To compare the horizontal continuity of the velocity structure in vertical section, we show the gradient direction and final inverted model along four main walk-away lines (Lines 1, 4, 7, and 10). Even though 2D and 3D FWI are conducted with the nearly similar FWI parameters, we observe significant differences in the gradient directions. For example, in 2D FWI, some artefacts caused from migration isochrone are strong at side of the model, which degrades the layer continuity. In addition, considering the line location in Figure 1, the azimuthal continuity of the layer is also not clear (Figures 4a and 4c). However, in 3D FWI results, migration isochrones and vertical noises around the borehole are significantly reduced compared to the first-iteration gradient direction of 2D FWI. As a result, the layer continuity along horizontal and azimuthal directions is significantly improved. The final inverted model using 3D FWI shows better features as a baseline model for future monitoring study.

Conclusions

In this study, we verify the suitability of 3D acoustic FWI in constructing a baseline model at CaMI-FRS project for a future monitoring study, focusing on the delineation of the target BBRS layer. We utilize the vertical component of walk-away and walk-around VSP data acquired at CaMI-FRS in 2018. As an objective function, we chose a global correlation norm in FWI to mitigate the influences of amplitude matching. Then, we compare the accuracy of 2D FWI and 3D FWI focusing on extremely thin target BBRS layer. Although we have successfully detected the BBRS layer in both 2D and 3D FWI results, the gradient direction and inverted models show significant differences considering geological structures of the area. In the 2D results, the continuity of velocity structures is not implemented well due to migration isochrones and strong noises around borehole. On the other hand, these issues are significantly addressed in 3D FWI by stacking more data from the azimuthal direction. These results indicate that 3D FWI can be a better tool than 2D FWI for time-lapse FWI.

Acknowledgements

The sponsors of CREWES are gratefully thanked for continued support. This work was funded by CREWES industrial sponsors and NSERC (Natural Science and Engineering Research Council of Canada) through the grant CRDPJ 543578-19. This work was also supported by the Korea Institute of Energy Technology Evaluation and Planning (KETEP) and the Ministry of Trade, Industry & Energy (MOTIE) of the Republic of Korea (No. RS-2023-00249135, 20212010200020). Data were acquired through a collaboration with the Containment and Monitoring Institute, Carbon Management Canada.

References

Cai, X., Innanen, K. A., Zhang, T., Hall, K. W., and Eaid, M., 2022, Analysis of the FWI workflow for geophone and DAS data from the 2018 CaMI VSP survey: CREWES Research Report, 34, 6.

Choi, Y., and Alkhalifah, T., 2012, Application of multi-source waveform inversion to marine streamer data using the global correlation norm: Geophysical Prospecting, 60, No. 4, 748-758.

Eaid, M., Keating, S., Innanen, K. A., Macquet, M., and Lawton, D., 2023, Field assessment of elastic full-waveform inversion of combined accelerometer and distributed acoustic sensing data in a vertical seismic profile configuration: Geophysics, 88, No. 6, 1ND-WC236.

Hall, K. W., Bertram, K. L., Bertram, M. B., Innanen, K. A., and Lawton, D. C., 2018, CREWES 2018 multi-azimuth walk-away VSP field experiment: CREWES Research Report, 30, 16.

Hu, Q., Eaid, M., Keating, S., and Innanen, K. A., 2022, Quantitative FWI characterization and monitoring of reservoir properties at the CMC Newell County Facility: CREWES Research Report, 34, 22.

Macquet, M., Lawton, D. C., Saeedfar, A. A., and Osadetz, K. G., 2019, A feasibility study for detection thresholds of CO2 at shallow depths at the CaMI Field Research Station, Newell County, Alberta, Canada: Petroleum Geoscience, 25, No. 4., 509-518.

Plessix, R.-E., 2006, A review of the adjoint-state method for computing the gradient of a functional with geophysical applications: Geophysical Journal International, 167, No. 2, 495-503.

Shin, C., Jang, S., and Min, D. J., 2001, Improved amplitude preservation for prestack depth migration by inverse scattering theory: Geophysical Prospecting, 49, No. 5, 592-606.

Tarantola, A., 1984, Inversion of seismic reflection data in the acoustic approximation: Geophysics, 49, No. 8, 1259-1266.

Xu, T., McMechan, G. A., and Sun, R., 1995, 3-D prestack full-wavefield inversion: Geophysics, 60, No. 6, 1805-1818.